ORCA – Online Research @ Cardiff

This is an Open Access document downloaded from ORCA, Cardiff University's institutional repository:https://orca.cardiff.ac.uk/id/eprint/101264/

This is the author's version of a work that was submitted to / accepted for publication.

Citation for final published version:

Pritchard, Manon F. , Powell, Lydia C. , Jack, Alison A., Powell, Kate , Beck, Konrad , Florance, Hannah, Forton, Julian, Rye, Philip D., Dessen, Arne, Hill, Katja E. and Thomas, David W. 2017. A low-molecular-weight alginate oligosaccharide disrupts pseudomonal microcolony formation and enhances antibiotic effectiveness. Antimicrobial Agents and Chemotherapy 61 (9) , e00762-17. 10.1128/AAC.00762-17

Publishers page: http://dx.doi.org/10.1128/AAC.00762-17

Please note:
Changes made as a result of publishing processes such as copy-editing, formatting and page numbers may not be reflected in this version. For the definitive version of this publication, please refer to the published source. You are advised to consult the publisher's version if you wish to cite this paper.

This version is being made available in accordance with publisher policies. See http://orca.cf.ac.uk/policies.html for usage policies. Copyright and moral rights for publications made available in ORCA are retained by the copyright holders.

A low molecular weight alginate oligosaccharide disrupts pseudomonal microcolony formation and enhances antibiotic effectiveness

Manon F. Pritchard,[a#] Lydia C. Powell,[a] Alison A. Jack,[a] Kate Powell,[a] Konrad Beck,[a] Hannah Florance,[b] Julian Forton,[c] Philip D. Rye,[d] Arne Dessen,[d] Katja E. Hill,[a] David W. Thomas[a]

Advanced Therapies Group, Cardiff University School of Dentistry, Cardiff, UK[a]; Department of Biosciences, College of Life and Environmental Sciences, Exeter University, Exeter, UK[b]; Childrens Hospital of Wales, Paediatric Respiratory Medicine, Cardiff, UK[c]; AlgiPharma AS, Sandvika, Norway[d]

Running Head: OligoG CF-5/20 disrupts pseudomonal microcolonies

#Address correspondence to Manon Pritchard, pritchardmf@cardiff.ac.uk.

Present address:

- Alison A. Jack, Cultech Limited, Port Talbot, UK.
- Hannah Florance, UK Centre for Mammalian Synthetic Biology, The King's Buildings, Edinburgh, UK.

ABSTRACT

In chronic respiratory disease the formation of dense, 3-dimensional 'micro colonies' by *Pseudomonas aeruginosa* within the airway plays an important role in contributing to resistance to treatment. An *in vitro* biofilm model of pseudomonal microcolony formation using artificial sputum (AS) medium was established to study the effects of low molecular weight alginate oligomers (OligoG CF-5/20) on pseudomonal growth, microcolony formation and the efficacy of colistin. The studies employed clinical cystic fibrosis (CF) isolates (n=3) and reference non-mucoid and mucoid multi-drug resistant (MDR) CF isolates (n=7). Bacterial growth, biofilm development and disruption were studied using cell-viability assays and image analysis using scanning electron- and confocal laser scanning microscopy. Pseudomonal growth in AS medium was associated with increased ATP production ($p<0.05$) and the formation (at 48 h) of discrete (>10 µm) microcolonies. In conventional growth medium, colistin retained an ability to inhibit growth of planktonic bacteria, although the MIC was increased (0.1 to 0.4 µg/ml) in AS medium versus. In contrast, in an established biofilm model in the AS medium, the efficacy of colistin was decreased. OligoG CF-5/20 ($\geq$2%) treatment however, induced dose-dependent biofilm disruption ($p<0.05$), and led to colistin retaining its antimicrobial activity ($p<0.05$). Whilst circular dichroism indicated that OligoG CF-5/20 did not change the orientation of the alginate carboxyl groups, mass-spectrometry demonstrated that the oligomers induced dose-dependent (>0.2%; $p<0.05$) reductions in pseudomonal quorum sensing signaling. These findings reinforce the potential clinical significance of microcolony formation in the CF lung, and highlight a novel approach to treat MDR pseudomonal infections.

Keywords: *Pseudomonas aeruginosa*, colistin, cystic fibrosis, alginate, OligoG CF-5/20

50 The opportunistic Gram-negative pathogen *Pseudomonas aeruginosa* is found in a range of
51 chronic human respiratory diseases, including chronic obstructive pulmonary disease and
52 cystic fibrosis (CF) (1). CF is a life-threatening, autosomal recessive genetic disorder
53 affecting 1 in 2,300 Caucasian live births (2). Reduced airway surface-liquid volume and
54 abnormally viscous sputum result in ineffective mucociliary clearance (3). Chronic bacterial
55 colonization of the lung by a number of opportunist pathogens occurs, most notably *P.*
56 *aeruginosa,* which will predominate with time (4).

57 Within the diseased lung, patho-adaptive mutation results in the selection of
58 hypermutator *P. aeruginosa* strains (5, 6). In *P. aeruginosa* this adaption occurs with a
59 switch to the mucoid phenotype, characterized by over-production of high molecular weight
60 (Mw; >15 kDa) alginate exopolysaccharide (EPS) (7, 8). This switch is accompanied by
61 modification of acyl homoserine lactone (AHL) and *Pseudomonas* quinolone signal (PQS)-
62 dependent quorum sensing (QS) systems (9), with altered production of virulence factors
63 e.g. pyocyanin and hydrogen cyanide (10). Extracellular alginate affords protection from
64 host innate immune-responses, including phagocytosis and neutrophil-derived reactive
65 oxygen species (11). Mucoidal pseudomonal strains are often un-responsive to aggressive
66 antibiotic selection (12) and 18.1% of CF patients are colonized with multi-drug resistant
67 (MDR) *P. aeruginosa* (13).

68 In contrast to standard laboratory models of bacterial biofilm formation on material
69 surfaces, biofilms within the CF lung form as non-adherent spherical microcolonies,
70 embedded in respiratory mucin (14, 15). Whilst *in vitro* studies of *P. aeruginosa* from CF
71 lungs routinely employ nutrient-rich media to optimize bacterial growth, or Mueller-Hinton
72 (MH) medium, such media fail to adequately reproduce the lung environment or secretome
73 (3). More recently, defined media such as artificial sputum (AS) medium (containing
74 components of CF sputum e.g. DNA, mucin, mineral salts, proteins and amino acids) have
75 been employed to model the behavior of *P. aeruginosa* (16-18). These AS medium models
76 have been used to study the adaptation of pathogens to the CF lung using whole-genome

77 sequencing and microarray expression profiling (19), analyze diffusion (20) and test the
78 effectiveness of antibacterial therapeutics (21).

79 This distinctive biofilm microcolony formation in the CF lung has been demonstrated *ex-*
80 *vivo* in freshly-excised intraluminal material and in lung sections (14). Studies have also
81 further shown that *in vitro* biofilms observed in nutrient-limited conditions are increasingly
82 recalcitrant to antibiotic therapy due to enhanced tolerance (22). The design and delivery of
83 antimicrobial therapy targeted against the polymicrobial respiratory biofilm is, therefore,
84 challenging (23).

85 The acquisition of MDR *Pseudomonas* in the CF lung has led to a resurgence of clinical
86 interest in the bacteriocidal antibiotic colistin (24). Overlooked for many years due to
87 associated nephro- and neuro-toxicity (25, 26), colistin is increasingly used to treat life-
88 threatening infections (24) and as an inhaled therapy in CF to prevent establishment of
89 infection by MDR bacteria (25). While resistance to colistin remains low (27), the emergence
90 of colistin-resistant strains heralds fears of a post-antibiotic era (28).

91 We previously described the use of a low molecular weight alginate oligomer (OligoG
92 CF-5/20, ≥ 85% guluronic acid, with a degree of polymerization [DPn] of 16; Mn 3,200) from
93 the seaweed *Laminaria hyperborea* as a promising novel therapy in CF (29-31). *In vitro*
94 studies, demonstrated the ability of OligoG CF-5/20 to modify bacterial surface charge (30)
95 and biofilm growth of non-mucoid *Pseudomonas* sp. in conventional culture/biofilm models
96 (29). It is however, important to determine whether OligoG CF-5/20 could modify bacterial
97 growth within the inherently antibiotic-resistant microcolonies, which characterize the
98 diseased CF lung.

99 The objective of this study was to investigate the therapeutic efficacy of OligoG CF-5/20
100 and colistin in an *in vitro* microcolony model. We characterized the growth of fresh clinical
101 isolates from CF patients and strains from the International *P. aeruginosa* Reference Panel
102 (IPARP). Planktonic and biofilm cultures of wild-type PAO1 and the mucoid MDR
103 NH57388A were studied in MH and AS media. We developed microcolonies in the AS
104 medium and investigated the ability of OligoG CF-5/20 to modify these biofilms and further

105 determined the effectiveness of a combination treatment with colistin. The effect of colistin
106 on the mucoid CF isolate NH57388A grown under planktonic and biofilm conditions was
107 reduced in this AS medium. In contrast, OligoG CF-5/20 retained its dose-dependent anti-
108 biofilm properties, as well as maintaining the effectiveness of colistin *in vitro*, demonstrating
109 that addition of alginate oligosaccharides modifies pseudomonal microcolony assembly.
110

111 **RESULTS**

112 **Non-mucoid *P. aeruginosa* IPARP have faster growth rates in MH medium than either**
113 **mucoid or new non-mucoid CF isolates**

114 Growth of non-mucoid *P. aeruginosa* in MH medium from the IPARP reference strains was
115 more abundant (maximum absorbance ≥1) compared to the delayed, weaker growth of the
116 fresh clinical isolates (maximum absorbance ≤1); acquiring stationary phase at 12 h versus
117 20 h respectively (**Fig. 1A**). The growth rates of the non-mucoid *P. aeruginosa* (PAO1, AA2,
118 AA44) were also greater than those of the new CF Isolates (22476, 22078, 22554) and those
119 of the mucoidal strains (AA43, IST27, 2192, NH57388A) from the IPARP collection (**Fig. 1B**)
120 having doubling-times (at maximum exponential growth) of 0.2-0.23 versus 0.31-0.6 versus
121 0.29-0.56 unit/h respectively.

122

123 **Colistin maintains its antimicrobial properties in the presence of the mucolytic OligoG**
124 **CF-5/20**

125 Initial studies on the effect of OligoG CF-5/20 and colistin (0.5x minimum inhibitory
126 concentration [MIC] value) on pseudomonal growth in MH medium, demonstrated no
127 difference in the growth rate of NH57388A when treated with colistin (0.16 unit/h) compared
128 to the control (**Fig. 1C**), although a reduced growth rate (0.12 unit/h) was noted when treated
129 with either 2% OligoG CF-5/20 or colistin with 2% OligoG CF-5/20. This was reflected by the
130 significantly decreased cell biomass at stationary phase (36 h) following treatment with 2%
131 OligoG CF-5/20 in combination with colistin compared to the control ($p<0.05$).

132 In the biofilm disruption assay, confocal laser scanning microscopy (CLSM) images of
133 LIVE/DEAD®-stained, 24 h established pseudomonal biofilms demonstrated homogenous
134 growth in the untreated control (**Fig. 1D**). Treatment for 1 h with colistin alone at 0.5x the
135 minimum biofilm eradication concentration (MBEC value as previously described [32]) was
136 associated with a decreased density of the resultant biofilm (**Fig. 1E**). Furthermore, when
137 treated with 2% OligoG CF-5/20 alone for 1 h, the biofilm height was reduced and there was

138 increased porosity (**Fig. 1F**). Combination treatment of colistin and 2% OligoG CF-5/20
139 resulted in marked biofilm disruption (**Fig. 1G**). Quantification using COMSTAT image
140 analysis software (33) revealed that biofilm height was significantly reduced from 11 ±4 μm
141 (in the untreated control) to 1.1 ±0.2 μm following 2% OligoG CF-5/20 and colistin
142 combination treatment (**Fig. 1H**). In parallel, the ratio of dead to live cells was significantly
143 increased following treatment with colistin (0.24 ±0.07) or 2% OligoG CF-5/20 and colistin in
144 combination (0.49 ±0.22) compared to the control (0.053 ±0.014; $p<0.05$; **Fig. 1I**); with
145 associated increases in porosity.

146

147 **Mucoid and non-mucoid *P. aeruginosa* show a distinctly altered biofilm phenotype**
148 **in artificial sputum medium**

149 Biofilms grown in different nutrient media exhibited distinct patterns of growth, with a marked
150 phenotypic difference in biofilm architecture in MH- versus AS medium (**Fig. 2A-B;**
151 diagrammatic representation **Fig. 2C**). Pseudomonal biofilms of both strains showed
152 conventional homogenous growth in MH medium, whilst discrete, spherical microcolonies
153 with an inter-linking network of extracellular polysaccharide (EPS) were apparent in AS
154 medium. Microcolonies were not strongly bound to the well plates and varied considerably
155 in size. The median diameter of the PAO1 and NH57388A microcolonies was 14 ± 4 μm
156 and 11 ±5 μm respectively; the difference in size perhaps reflecting the slower growth rate of
157 the mucoid strain. Elongated structures between the microcolonies were composed of
158 linearly arranged bacterial cells.
159 Growth curves were performed using a cell-viability assay, (measuring ATP production);
160 conventional growth curves with optical density measurements being impractical in AS
161 medium, due to bacterial aggregation and microcolony formation. Marked differences in
162 ATP production between cells grown in AS versus MH medium were evident within 24 h,
163 being considerably elevated in AS medium (**Fig. 2D**).

164

165 **OligoG CF-5/20 disrupts *P. aeruginosa* (NH57388A) microcolony formation in artificial**
166 **sputum medium**

167 SEM studies using a biofilm formation assay of *P. aeruginosa* (NH57388A) biofilms grown in
168 MH medium ± OligoG CF-5/20 demonstrated the growth inhibitory effects of OligoG CF-5/20
169 at ≥2% (w/v; **Fig. 3A**), which was reflected in a corresponding reduction in EPS formation.
170 Mucoid *P. aeruginosa* (NH57388A) formed typical microcolonies in AS medium at 48 h (**Fig.**
171 **3B**); with individual bacterial cells visible on the surface of the microcolonies encased in EPS
172 (**Fig. 3C**). Biofilm formation in the presence of OligoG CF-5/20 was associated with a dose-
173 dependent decrease in microcolony size and increasing cellular disruption of the biofilms. At
174 6% OligoG CF-5/20, the median microcolony diameter was 4.5 µm versus 6.6 µm in the
175 untreated control (**Fig. 3D**). Corresponding CLSM images of Syto-9 and Concanavalin A
176 633 matrix-stained NH57388A 48 h biofilms in AS medium showed dense microcolonies
177 surrounded by EPS (red) throughout the structure (**Fig. 3E**). Biofilms grown in OligoG CF-
178 5/20 exhibited a decreased, overall biofilm mass with few spherical microcolonies and
179 reduced EPS.

180 Using the biofilm disruption assay, CLSM images of matrix-stained NH57388A 48 h-
181 established biofilms stained with Syto-9 (green) demonstrated large cellular aggregates or
182 microcolonies (**Fig. 3F**) on (or within) a layer of cells. Treatment for 1 h with 2% OligoG CF-
183 5/20, induced a reduction in aggregate size (**Fig. 3G**), with marked microcolony disruption.
184 3D videos of these images are available online (**Supplementary information Video 1**).

185

186

187 **Circular dichroism spectra of OligoG CF-5/20 mixed with high molecular weight**
188 **pseudomonal alginate do not indicate a specific interaction**

189 Circular dichroism (CD) spectroscopy was used to test whether OligoG CF-5/20 and the high
190 molecular weight EPS alginate produced by mucoid pseudomonal strains show a specific

191 interaction. The CD chromophore responsible for the Cotton effect observed at ca. 210 nm
192 has been identified as the carboxyl groups of the alginates, and the n → π* transition reflects
193 their orientation (34). Upon heating from 4 to 37°C, spectra of high Mw alginate showed no
194 changes over a period of ~80 min (**Fig. 4A**, scans 1 to 7). Subsequent addition of OligoG
195 CF-5/20 at a 50-fold molar excess resulted in an increased CD amplitude, i.e. more negative
196 values (**Fig. 4A**, scans 8 to 11). Addition of Ca^{2+} to a final concentration of 1 mM had no
197 effect (**Fig. 4A**, scans 12 to 17). The spectra observed for the high Mw alginate/OligoG CF-
198 5/20 mixture corresponded to an additive effect of the two components not indicating any
199 change in the orientation of the carboxyl groups (cf. dashed curves in **Fig. 4A**). Experiments
200 in which Ca^{2+} was added to the high Mw alginate before the addition of OligoG CF-5/20, and
201 a 1:600 molar ratio of high Mw alginate to OligoG CF-5/20 also are compatible with an
202 additive effect with no indication of a change in the orientation of the carboxyl groups (**Fig.
203 S1**).
204

205 **OligoG CF-5/20 affects cell-signaling in pseudomonal biofilms**

206 To determine whether OligoG CF-5/20 affected these changes via modification of QS
207 signaling in the biofilm systems, liquid chromatography/mass spectrometry (LC/MS) was
208 employed to detect the pseudomonal signaling molecules, C4- and 3-oxo-C12-acyl
209 homoserine lactones (AHLs). AHL levels were determined at 30 and 48 h for PAO1 cells
210 grown in both MH and AS medium. Initial experiments compared growth in MH and AS
211 medium at 30 h (as at earlier time points in AS medium, AHLs were at the limits of detection;
212 results not shown). LC/MS values indicated a reduction in the production of both 3-oxo-C12-
213 AHL and C4-AHL signaling molecules in AS medium (62 and 783 fold respectively)
214 compared to MH medium (**Fig. 4B**). Further experiments were performed on OligoG CF-
215 5/20-treated cultures grown in AS medium for 30 and 48 h (corresponding to mid- and late-
216 stationary phase respectively; results not shown). Interestingly, in this model it was evident
217 that OligoG CF-5/20 (0.2-2%) induced a dose-dependent decrease in 3-oxo-C12 AHL
218 (produced by the Las pathway) in comparison to the control at 30 and 48 h (**Fig. 4C**), but did

219 not induce any significant change in C4-AHL (produced by the RhlI pathway; **Fig. 4D**).
220 Although OligoG CF-5/20 had a significant effect on biofilm formation, there was no marked
221 difference in ATP production (cell viability) by PAO1 or NH57388A following treatment (**Fig.**
222 **4E and 4F**).
223

224 **The antibiotic properties of colistin were retained in artificial sputum medium when**
225 **combined with OligoG CF-5/20**

226 Assays of biofilm disruption in established (24 h) non-mucoid (PAO1) and mucoid
227 (NH57388A) pseudomonal biofilms following 24 h treatment with OligoG CF-5/20 and/or
228 colistin were investigated in AS medium. The observed MIC value for colistin was 4x greater
229 in AS medium (0.4 µg/ml versus 0.1 µg/ml) compared to MH medium. The MIC employed in
230 subsequent studies was based upon these findings.
231 As observed previously, PAO1 and NH57388A demonstrated the formation of large
232 numbers of spherical microcolonies, with extensive EPS in this model (**Fig. 5A, 5B**). The
233 mucoidal NH57388A biofilms were characterized by smaller microcolonies when compared
234 to PAO1 (median diameter 11 µm versus 14 µm respectively) (**Fig. 5C, 5D)**. Biofilm
235 treatment with colistin (at x4 the MBEC value (32), induced disruption of PAO1 and
236 NH57388A bacterial networks. The microcolonies, however, remained intact (with no
237 change in median diameter; $p>0.05$). In contrast, treatment with 2% OligoG CF-5/20
238 induced significant decreases in the median microcolony diameter (6.9 ±2.0 µm and 6.1 ±2.7
239 µm; PAO1 and NH57388A respectively; $p<0.05$) characterized by marked disruption of the
240 inter-colony networks and microcolony morphology. Combining OligoG CF-5/20 with colistin
241 (although not as effective as OligoG CF-5/20 alone on the mucoid strain) effectively
242 disrupted both microcolony structure (reducing the median diameter by 60% in PAO1) as
243 well as the inter-colony branching/bridging in both mucoid and non-mucoid models. Overall
244 structural differences can be seen at a lower magnification in **Fig. S2.**
245

246

247 **DISCUSSION**

248 The improved survival of CF patients, due in part to the chronic administration of antibiotics,
249 has compounded the problems associated with resistance to antibiotic treatment (35, 36).
250 With the rapid emergence of antibiotic resistance, the development of new therapies is
251 essential. Increased antibiotic resistance in biofilms has been extensively described, with
252 biofilms shown to resist antibiotics by up to 1000 fold (37). These studies demonstrate the
253 potential benefits of combination therapies using a novel mucolytic alongside conventional
254 antibiotics in the treatment of antibiotic-resistant, microcolony-forming *Pseudomonas* sp.
255 lung Infections.

256 The resurgence of interest in colistin, a highly-effective membrane-permeabilizing
257 antibiotic, reflects the failure of conventional antibiotics in MDR infections (25).
258 Unfortunately, the emergence of plasmid-mediated colistin resistance provides the imminent
259 possibility for horizontal gene transfer from veterinary to human pathogens (38). Due to the
260 high rate of MDR in *P. aeruginosa* (39) colistin is now regarded as an antibiotic of 'last resort'
261 and its use (in non-CF patients) is therefore limited to prevent further development of
262 resistance (40).

263 Colistin acts through positively-charged electrostatic interactions with the negatively-
264 charged bacterial lipopolysaccharide (LPS), facilitating membrane disruption. The observed
265 lowering of the efficacy of colistin in AS medium may, therefore, not only relate to an altered
266 growth rate in this environment, (which mimics growth conditions in the CF lung), but also
267 may be due to LPS modification and/or direct binding by mucin in the AS medium, effectively
268 'sequestering' free antibiotic (41). This EPS effect, and the apparent differences in MIC for
269 colistin-treated NH57388A, (with MIC values being 4X greater in AS versus MH medium)
270 reflect the 10^4-fold difference previously observed between MIC (0.094 μg/ml) and MBEC
271 (>512 μg/ml) values for NH57388A *in vitro* (42).

272 Within the diseased CF lung, >95% of *P. aeruginosa* exist in dense microcolonies, >5
273 µm from the epithelial cell-surface and independent of cell-surface attachment (14, 43). The
274 microcolonies develop in the early stages of lung infection and readily resist physical
275 disruption (43). The AS medium employed here induced pseudomonal microcolony
276 formation in both non-mucoid and mucoid strains as seen previously. These microcolonies
277 resembled those observed in a range of CF epidemic and non-epidemic *P. aeruginosa*
278 strains (16); SEM demonstrating bridges between the microcolonies which appeared to be
279 composed of elongated single-cells encased in EPS, as previously observed in flow-cell
280 systems (44). OligoG CF-5/20 was able to modulate both the size and structure of these
281 bacterial microcolonies. This may relate to its ability to interact with the EPS component of
282 the biofilm, by direct effects on the pseudomonal bacterial cell-surface, and on bacterial
283 growth (29, 30). Whilst imaging studies demonstrated that colistin effectively disrupted the
284 inter-colony bridges, the microcolonies (which were encased in EPS) appeared unaffected
285 by colistin alone.

286 Despite the possible charge interactions between the cationic peptide colistin (41)
287 and the anionic OligoG CF-5/20 (30), colistin retained its antibiotic activity in the presence of
288 OligoG CF-5/20. The ability of OligoG CF-5/20 to modify biofilm assembly in *Pseudomonas*
289 spp. has previously been attributed to irreversible binding at the bacterial cell surface (30).
290 Moreover, the ability of OligoG CF-5/20 to potentiate the effectiveness of colistin against
291 mucoid NH57388A biofilms by OligoG CF-5/20 has recently been demonstrated in MBEC
292 assays (32).

293 In this model, the ability of OligoG CF-5/20 (both alone, and more markedly with
294 colistin) to effectively disrupt the EPS of established biofilms was clearly evident. Disruption
295 of the tight EPS-network, which comprises >90% of the biofilm dry-weight (45), has been
296 shown to lead to less mechanically-stable biofilms, which are then more susceptible to
297 antibiotics (46). It appears therefore that EPS disruption by OligoG CF-5/20 maintained the
298 antimicrobial action of colistin by reducing its ability to bind to components of the biofilm

299 matrix, thereby increasing its penetration through the biofilm, facilitating access of colistin to
300 the pseudomonal cell membrane.

301 Initial experiments demonstrated the contrasting growth phenotype between freshly
302 isolated clinical strains compared to the well-characterized reference strains. Compensatory
303 mutations in the clinical CF isolates are thought to provide differential fitness benefits, which
304 are advantageous within the CF lung environment (47). Fitness 'trade-offs', where beneficial
305 adaptations that improve fitness under one environmental condition that may lead to
306 compensatory loss of other traits have been described (48). This may, in part, explain the
307 observed lower growth rate of fresh clinical isolates (adapted to the CF lung) when
308 compared to the laboratory-maintained IPARP CF strains. This variability highlights the
309 importance of utilizing the reference strain collection for therapeutic development to ensure
310 global standardization of *in vitro* testing.

311 A number of approaches have been attempted to modify biofilm EPS and facilitate
312 treatment or displacement therapy. These have included: use of bacterial polysaccharides
313 e.g. from marine *Vibrio* sp. (49); co-administration of alginate lyase with DNase, which has
314 been reported to increase the efficacy of antibiotics in reducing biofilm growth (50) and co-
315 administration of antibiotics with alginate lyase to eliminate mucoid variants not affected by
316 antibiotics alone (51). Interestingly, we have also previously demonstrated synergy between
317 OligoG CF-5/20 and rhDNase I in modifying the mechanical and structural properties of CF
318 sputum (31).

319 Biofilms also contain bacterially-derived alginates which, in contrast to OligoG CF-5/20,
320 lack G-blocks and have a considerably higher molecular mass (52). Anionic EPS
321 components, such as carboxyl groups, interact strongly with multivalent cations such as
322 Ca^{2+}, resulting in robust biofilms (53). Sletmoen et al., (2012) demonstrated that alginate
323 oligomers may destabilize the interaction between high Mw bacterially-produced alginates
324 and mucin. The ionic displacement of divalent cations e.g. Ca^{2+} has been described as a
325 mechanism by which antimicrobial cationic peptides can potentiate antibiotics (54).
326 Similarly, the anionic alginate G-blocks may displace divalent cations associated with the

327 biofilm, resulting in a weaker biofilm structure. CD spectroscopy has previously been used
328 to investigate the structural and conformational changes of polysaccharides containing
329 uronic acid residues, and has recently been employed to characterize homopolymeric
330 fractions of the linear co-polymers L-guluronate and D-mannuronate (34, 55). The gelation
331 of alginate in the presence of divalent cations such as Ca^{2+} in homopolyguluroinc acid is
332 known to induce changes in the coordination of the carboxylate groups (56). However, CD
333 spectra indicated that the orientation of the carboxy groups monitored at ~210 nm were not
334 changed upon mixing OligoG CF-5/20 with high Mw alginate.

335 Previous studies in planktonic systems demonstrated that OligoG CF-5/20 modified both
336 *pilE* gene expression and bacterial motility in *Pseudomonas aeruginosa* (30), which are
337 controlled by QS. The finding that levels of *P. aeruginosa* AHL signaling molecules were
338 significantly reduced in AS medium compared to MH medium was perhaps unsurprising,
339 reflecting the change in growth/morphology. Sriramulu et al (2005), demonstrated the
340 importance of *lasR* for the formation of the dense microcolony phenotype and these data
341 demonstrated the ability of (≥2%) OligoG CF-5/20 to significantly reduce 3-oxo-C12-AHL
342 production at both mid- and late-stationary phase growth (30 and 48 h). The lack of an
343 observed effect on the Rhl product, C4-AHL, may reflect the reduced expression of *rhlR*
344 which is known to occur in AS medium (16).

345 These experiments demonstrate that the previously described antibacterial effects of
346 OligoG CF-5/20, are evident in this pseudomonal microcolony assay system which more
347 closely resembles growth in the CF lung. It must be remembered that many of the
348 components of the *in vivo* lung are absent in the biofilm model, including lactoferrin, lipids
349 and oligopeptides, which may modulate bacterial behavior *in vivo*. OligoG CF-5/20 was
350 shown to disrupt the biofilm EPS network and, in combined respiratory therapies, this
351 inhaled treatment may facilitate increased access of therapeutic agents to bacteria and/or
352 the lung cell-surface. The mechanistic studies showed that this disruption of EPS structure
353 was not simply related to interaction between the OligoG CF-5/20 and the pseudomonal (M-
354 block alginate), but may rather reflect modification of QS signaling within the biofilm. The

355 findings here, and the proven safety of the agent as an inhalational therapy
356 (www.clinicaltrials.gov, Identifier: NCT00970346 and NCT01465529), highlight the potential
357 utility of this agent in the treatment of MDR bacterial infections in a range of human
358 diseases. Phase IIb human studies are currently ongoing (www.clinicaltrials.gov, Identifier:
359 NCT02157922 and NCT02453789).
360
361
362 **METHODS**
363 **Bacterial strains and media**
364 *P. aeruginosa* strains were cultured on blood agar plates and grown overnight in Tryptone
365 soy broth (TSB; LabM), at 37°C. Mueller Hinton (MH) medium or Artificial Sputum (AS)
366 medium (adapted from earlier studies [43] by supplementation with 20 ml/L RPMI 1640 as
367 an amino acid source; Sigma Aldrich) were also employed.
368 Reference strains (n=7) were obtained from the International *P. aeruginosa*
369 Reference Panel (IPARP) (57) including: AA2 and AA44 (early and late non-mucoid CF
370 colonizers respectively); AA43 (mucoidal colonizer from the same AT code) and mucoidal
371 CF isolates, IST 27 (Lisbon, Portugal) and 2192 (source ID; Boston, MA). The well
372 characterized non-mucoid PAO1 and mucoidal MDR CF strain NH57388A (Copenhagen,
373 Denmark), were also used in subsequent experiments.
374
375 **Patients and clinical isolates**
376 Newly isolated, non-mucoid *P. aeruginosa* strains (22078, 22554, and 22476) were obtained
377 from induced sputum collected from children attending the Cystic Fibrosis Unit at the
378 University Hospital of Wales, Cardiff participating in the Sputum Induction Trial (SpIT) study
379 (a longitudinal sputum collection study in CF patients; LREC approved [project ID
380 11/RPM/5216]).
381

382 **Changes in antibiotic susceptibility in the different media**

383 Bacteriocidal values for colistin in MH and AS medium were studied using standard
384 minimum inhibitory concentration (MIC) assays as previously described (29).

385

386 **Effects of OligoG CF-5/20 on pseudomonal growth in the presence of colistin**

387 For the inoculum for the pseudomonal growth curves, overnight cultures in TSB (n=3) were
388 standardized to 10^6 cells/ml in MH medium. For treated samples, *P. aeruginosa*
389 (NH57388A; n=3) standardized to 10^8 cells/ml in MH medium were treated with and without
390 2% OligoG CF-5/20 (w/v) ± colistin (0.5x MIC; 0.05 µg/ml). Samples were grown (24 h;
391 37°C) in 96-well plates and change in cell density recorded every hour (OD_{600}) on a
392 FLUOstar Omega plate reader. Cell doubling time was calculated for each growth curve.

393

394 **Viable microbial cell numbers in culture when treated with OligoG CF-5/20**

395 Adenosine triphosphate (ATP) production by PAO1 and NH57388A was compared in MH
396 and AS medium ± 2% OligoG CF-5/10. Cultures were prepared as for the growth curve
397 experiments and analyzed using the BacTiter-Glo™ Microbial Cell Viability Assay (Promega)
398 at 0, 2, 4, 6, 8, 12, 24 and 48 h with luminescence read on a FLUOstar Omega plate reader.

399

400 **Confocal laser scanning microscopy biofilms in MH and AS media in the presence of**
401 **OligoG CF-5/20**

402 Pseudomonal cultures (NH57388A) standardized to 10^7 cfu/ml, were inoculated 1:20
403 in MH or AS media and incubated (37°C; 20 rpm) for 24 h or 48 h respectively in Greiner
404 glass-bottomed optical 96-well plates; the difference in growth rates in the two media,
405 accounting for the longer growth time used for the AS medium. For antimicrobial treatment,
406 half of the supernatant was gently removed and replaced with fresh MH or AS medium ± 2%
407 OligoG CF-5/20 and/or colistin at half the MBEC (2 µg/ml) and incubated for 1 h.

408 Supernatant was then removed and replaced with 6% (v/v) LIVE/DEAD® (Invitrogen) stain in
409 PBS prior to imaging. CLSM was performed using a Leica SP5 confocal microscope with
410 x63 magnification under oil. Z-stack CLSM images were analyzed using COMSTAT image
411 analysis software (33).

412 AS medium biofilms were also fixed overnight at 4°C with 3% (v/v) glutaraldehyde
413 and stained (1 h) at room temperature with 0.15% Syto-9 (Invitrogen) in PBS. CLSM of Z-
414 stack images was achieved using sequential fluorescence recordings of Syto-9 ($\lambda_{ex}/\lambda_{em}$ max:
415 $480/500_{nm}$) and propidium iodide ($\lambda_{ex}/\lambda_{em}$ max: $490/635_{nm}$).

416 For EPS imaging, NH57388A biofilms (48 h) were grown in AS medium in 12-well
417 glass bottomed plates (No. 1.5; MatTek Corp. Ashland, MA, USA) ± 2 or 6% OligoG CF-
418 5/20.. Biofilms were fixed with 2.5% glutaraldehyde in PBS overnight at 4°C. Fixative was
419 then removed and biofilms stained with Syto-9 (0.15% in PBS) and Concanavalin A, Alexa
420 Fluor™ 633 Conjugate (100 μg/ml in PBS; Invitrogen) prior to CLSM imaging.

421

422 **Scanning electron microscopy of OligoG CF-5/20 treated biofilms in different media**

423 *P. aeruginosa* (PAO1 and NH57388A) cultures were adjusted to 10^7 cfu/ml in MH or AS
424 medium and grown (37°C for 24 h or 48 h respectively at 20 rpm) in 12-well plate (Greiner
425 Bio-One) on Thermanox™ glass slides (Agar Scientific) ± OligoG CF-5/20 0.2%, 2% or 6%
426 (w/v). For the established (24 h) biofilm model, half the supernatant was gently removed
427 and replaced with 2% OligoG CF-5/20 (v/v), colistin (x4 MBEC; 16 μg/ml), or combination
428 treatment and incubated for 24 h. Supernatant was removed and biofilms fixed with 2.5%
429 (v/v) glutaraldehyde prior to being washed (x4) with dH_2O and freeze-dried. The samples
430 were then gold-coated and imaged using a Tescan Vega conventional SEM (2.5 kV) for
431 untreated samples and the established biofilm model or performed using a Hitachi S4800 (1
432 kV) scanning electron microscope (SEM) for the biofilm development model. Pseudo-
433 coloring of SEM images was performed using Adobe Photoshop CS6 (Adobe Systems

434 Europe Ltd, Maidenhead, UK). ImageJ was used to measure microcolony diameter
435 following line calibration using the known set scale for each image. Measurements of the
436 three largest cellular aggregates in each image were taken at the narrowest diameter.

437

438 **Direct interaction of OligoG CF-5/20 and pseudomonal high molecular weight alginate**
439 **using circular dichroism spectroscopy**

440 CD spectra of OligoG CF-5/20, high Mw alginate (approx. 100 kDa) comprising 7% guluronic
441 acid derived from *Pseudomonas aeruginosa*, and mixtures thereof were recorded using an
442 Aviv Model 215 instrument (Aviv Biomedical, Lakewood, NJ, U.S.A.). Samples were
443 dissolved in 100 mM NaCl, 5 mM Tris.Cl, pH 7.5, spun at 14,000 *g* for 30 min at 4°C, and
444 the supernatant transferred to a 0.1-cm quartz cell pre-warmed to 37°C. Repetitive spectra
445 were collected from 245 to 196 nm at 0.2 nm intervals with 2 s accumulation per point
446 corresponding to ~11 min/spectrum). Buffer baselines were subtracted and ellipticities (Θ)
447 were corrected for dilutions.

448

449 **Changes in quorum sensing acyl-homoserine lactone (AHL) production in different**
450 **media when treated with OligoG CF-5/20**

451 Overnight cultures of *P. aeruginosa* PAO1 were diluted (1:100) in either MH or AS medium
452 and grown for a further 30 or 48 h ± 0.2 or 2 % OligoG CF-5/20. Cultures were washed (x3;
453 18,000 *g*, 20 min, 4°C) in ice cold 0.9% NaCl and pelleted cells were dried (80°C) for 24 h
454 and weighed. Culture supernatants were vigorously mixed (30 s) in equal volumes of ethyl
455 acetate (acidified with 0.5% formic acid), and the upper layer collected (x3). The resultant
456 ethyl acetate fractions were allowed to evaporate and the precipitate was re-suspended in 1
457 ml of distilled H_2O (58). Samples were freeze-dried prior to analysis. Quantification of acyl

458 homoserine lactones was done using high performance liquid chromatography triple
459 quadrupole mass spectrometry (LC-QQQ-MS).
460 Freeze-dried samples were maintained on ice and reconstituted in acetonitrile (200
461 µl) with 0.1% acetic acid and 7.2 ng ml^{-1} of the internal standard umbelliferone. Samples
462 were centrifuged (16,100 *g*, 10 min, 4°C) and supernatants filtered (0.4 µm; x2). Samples (5
463 µl) were loaded onto a C18 XDB Eclipse (1.8 µm, 4.6 x 50 mm) reverse phase column and
464 quantified using a 1200 series HPLC coupled to a 6410B enhanced sensitivity triple
465 quadrupole (QQQ) mass spectrometer (Agilent Technologies, Palo Alto, USA). For
466 detection using positive ion mode, mobile phase A comprised of 5 mM ammonium acetate in
467 water modified with 0.1% acetic acid and B was acetonitrile containing 0.1% acetic acid.
468 The column was equilibrated in 2% B before increasing in a linear fashion to 100% over 6
469 mins. 100% B was maintained for a further 2 min before column re-equilibration. The
470 column temperature was maintained at 35°C for the duration with a flow rate of 0.3 mL/min.
471 Source parameters were set as follows: Temperature, 350°C; gas flow, 10 L/min; nebulizer,
472 35 psi; and capillary voltage, 4 kV. Data was analysed using Agilent MassHunter QQQ
473 Quantitative Analysis software (Version B.07.00). Peak areas were normalized to the
474 internal standard umbelliferone and concentrations calculated using standard concentration
475 curves, offset against blank values (the average peak areas for the blanks).

476

477 **Statistical analysis**

478 The COMSTAT data was normally distributed so a standard t-test was performed using
479 MiniTab 17 (Minitab Ltd, Coventry, UK) and a Bonferroni correction. A one-way ANOVA was
480 used for the AHL data using GraphPad 3 (La Jolla, CA, USA). STATA was used to carry out
481 a Kruskal-Wallis non-parametric test supplemented using Dunn's test for the microcolony
482 SEM measurements.

483

484 **ACKNOWLEDGEMENTS**

485 This study was supported by funding from the European Union via the Eurostars (TM)
486 Programme and the European Social Fund, Research Council of Norway, Cystic Fibrosis
487 Foundation US and AlgiPharma AS. We thank Professor N. Høiby for *P. aeruginosa* strain
488 NH57388A and Debbie Salmon for technical support for the LC/MS. We thank Professor
489 Gudmund Skjåk-Bræk for providing the high Mw pseudomonal alginate for the CD
490 studies. We would also like to thank Dr Damian Farnell for his support with the statistical
491 analysis. D.W.T. has a consultancy relationship and has, with K.E.H., received research
492 funding from AlgiPharma AS. A.D and P.D.R. are director/owners of AlgiPharma AS. The
493 other authors have no conflicts of interest to disclose.

494

495 **FIGURE LEGENDS**

496 **FIG 1** Comparison of planktonic growth in MH medium of characterized and new cystic
497 fibrosis *P. aeruginosa* isolates and biofilm growth following antimicrobial treatment. Growth
498 curves (24 h) of (A) Non-mucoid IPARP isolates (red) versus fresh clinical SpIT isolates
499 (blue) and (B) non-mucoid IPARP isolates (red) versus mucoid (green). (C) Growth curves
500 of NH57388A (36 h) ± 2% and OligoG CF-5/20 with/without colistin (0.05 µg/ml). Biofilm
501 disruption assay showing LIVE/DEAD® CLSM [scale bar 20 µm] of 24 h established
502 NH57388A biofilms, (D) untreated control, (E) 1 h colistin treatment, (F) 2% OligoG CF-5/20,
503 (G) combined treatment. COMSTAT analysis showing (H) mean height of biofilm and (I)
504 ratio of DEAD: LIVE cells. (*$p<0.05$)

505

506 **FIG 2** Comparison of growth of non-mucoid PAO1 and mucoid NH57388A *P. aeruginosa* in
507 Mueller-Hinton (MH) and artificial sputum (AS) medium. Scanning electron microscopy of
508 bacterial growth in MH (24 h) and AS medium (48 h; scale bar 20 µm), with corresponding
509 'zoomed-in' images in AS medium [scale bar 10 µm] (A) PAO1 and (B) NH57388A. (C)

510 Diagrammatic representation of biofilm structure in both media. (D) Cell viability (ATP
511 production) of *P. aeruginosa* NH57388A and PAO1 (10^8 cfu/ml) grown in MH and AS
512 medium.
513
514 **FIG 3** Biofilm formation assays showing mucoid NH57388A *P. aeruginosa* biofilms grown in
515 Mueller-Hinton (MH) and artificial sputum (AS) medium. SEM images of *P. aeruginosa*
516 (NH57388A) biofilms grown ±OligoG CF-5/20 for (A) 24 h in Mueller Hinton (MH) medium;
517 10 µm; (B), (C [zoomed in]) 48 h ± OligoG CF-5/20 [scale bar 5 µm] with (D) corresponding
518 scatter graphs showing approx. mean microcolony size. (E) Corresponding CLSM EPS
519 staining of *P. aeruginosa* (NH57388A) 48 h biofilms in artificial sputum (AS) medium using
520 Syto-9 (green) and Concanavalin A 633 (red). (F,G) Biofilm disruption assay using Syto-9
521 (green) showing cross-sectional views of 48 h established biofilms treated l h with 2%
522 OligoG CF-5/20 [scale bar 10 µm]. (*$p<0.05$).
523
524 **FIG 4** Effect of OligoG CF-5/20 on high Mw alginate and on cell signaling molecules *in vitro*.
525 (A) Circular dichroism (CD) spectra of high Mw pseudomonal alginate mixed with OligoG
526 CF-5/20. Scans 1-7 show spectra of high Mw alginate (~20 µM) followed over ~77 min upon
527 heating from 4 to 37^0C; scans 8-11 (~44min) are recorded after addition of OligoG CF-5/20
528 (850 µM) followed by addition of Ca^{2+} (1mM) (scans 12-17, ~ 66min). Spectra of OligoG CF-
529 5/20 (850 µM) alone and its sum with high Mw alginate (20 µM) are shown as black and red
530 dashed lines, respectively. High performance liquid chromatography (HPLC) mass
531 spectrometry (LC-QQQ-MS) to quantify acyl homoserine lactone (AHL; 3-oxo-C12-AHL and
532 C4-AHL) production of *P. aeruginosa* PAO1 (B) grown in MH and AS medium (30 h), and in
533 a time course assay (30 and 48 h) showing the effect of OligoG CF-5/20 on (C) 3-oxo C12-
534 AHL and (D) C4-AHL (*$p<0.05$; n=3). Cell viability (ATP production) over 48 h of (E) PAO1
535 and (F) NH57388A grown in MH and AS medium ± 2% OligoG CF-5/20 (2%G).
536

537 **FIG 5** Biofilm disruption assays showing scanning electron microscopy (SEM) of
538 antimicrobial (OligoG CF 5/20 and colistin) treated biofilms grown in ASM [Scale bar 10 µm].
539 SEM images of established (24 h) *P. aeruginosa* (A) PAO1 and (B) NH57388A biofilms
540 treated for 24 h with 2% OligoG CF-5/20 ± colistin (16 µg/ml) with corresponding median
541 microcolony diameter measurements for (C) PAO1 and (D) NH57388A (*$p<0.05$).
542

543 **Supplementary Figures**

544 **FIG S1** CD spectra of high Mw pseudomonal alginate mixed with OligoG CF-5/20. Scans 1-
545 2 show spectra of high Mw alginate (~20 µM) followed over ~22 min after heating from 4 to
546 37°C, after which Ca^{2+} was added (scans 3-8: c_{final} = 1mM; scans 9-11: c_{final} = 2mM). Oligo
547 G CF-5/20 was added to c_{fin} = 700µM (scans 12-15; molar ratio high Mw alginate to OligoG
548 CF-5/20 1:50) and c_{fin} = 4.2mM (scans 16-22; molar ratio high Mw alginate to OligoG CF-
549 5/20 1:600). Adding calcium to c_{fin} = 9 mM results in spontaneous alginate precipitation
550 (scans 23-25).
551

552 **FIG S2** Biofilm disruption assay showing SEM images of established (24 h) *P. aeruginosa*
553 (A) PAO1 and (B) NH57388A biofilms treated for 24 10 h with 2% OligoG CF-5/20 ± colistin
554 (16 µg/ml). Scale bar 20 µm.
555

556 **REFERENCES**

557 1. Valderrey AD, Pozuelo MJ, Jimenez PA, Macia MD, Oliver A, Rotger R. 2010.
558 Chronic colonization by *Pseudomonas aeruginosa* of patients with obstructive lung
559 diseases: cystic fibrosis, bronchiectasis, and chronic obstructive pulmonary disease.
560 Diagn Microbiol Infect Dis 68:20-27.
561 2. Farrell PM. 2008. The prevalence of cystic fibrosis in the European Union. J Cyst
562 Fibros 7:450-453.

563 3. Rubin BK. 2009. Mucus, phlegm, and sputum in cystic fibrosis. Respir Care 54:726-
564 732.
565 4. Li ZH, Kosorok MR, Farrell PM, Laxova A, West SEH, Green CG, Collins J, Rock MJ,
566 Splaingard ML. 2005. Longitudinal development of mucoid *Pseudomonas aeruginosa*
567 infection and lung disease progression in children with cystic fibrosis. JAMA 293:581-
568 588.
569 5. Marvig RL, Johansen HK, Molin S, Jelsbak L. 2013. Genome analysis of a
570 transmissible lineage of *Pseudomonas aeruginosa* reveals pathoadaptive mutations
571 and distinct evolutionary paths of hypermutators. Plos Genet 9,
572 doi:10.1371/journal.pgen.1003741.
573 6. Feliziani S, Marvig RL, Lujan AM, Moyano AJ, Di Rienzo JA, Johansen HK, Molin S,
574 Smania AM. 2014. Coexistence and within-host evolution of diversified lineages of
575 hypermutable *Pseudomonas aeruginosa* in long-term cystic fibrosis infections. Plos
576 Genet 10, doi:10.1371/journal.pgen.1004651.
577 7. Marvig RL, Sommer LM, Molin S, Johansen HK. 2015. Convergent evolution and
578 adaptation of *Pseudomonas aeruginosa* within patients with cystic fibrosis. Nature
579 Genet 47:57-64.
580 8. Bales PM, Renke EM, May SL, Shen Y, Nelson DC. 2013. Purification and
581 characterization of biofilm-associated EPS exopolysaccharides from ESKAPE
582 organisms and other pathogens. Plos One 8, doi:10.1371/journal.pone.0096166.
583 9. Ryall B, Carrara M, Zlosnik JEA, Behrends V, Lee X, Wong Z, Lougheed KE,
584 Williams HD. 2014. The mucoid switch in *Pseudomonas aeruginosa* represses
585 quorum sensing systems and leads to complex changes to stationary phase
586 virulence factor regulation. Plos One 9, doi:10.1371/journal.pone.0096166.
587 10. Ryall B, Davies JC, Wilson R, Shoemark A, Williams HD. 2008. *Pseudomonas*
588 *aeruginosa*, cyanide accumulation and lung function in CF and non-CF
589 bronchiectasis patients. Eur Resp J 32:740-747.

590 11. Leid JG, Willson CJ, Shirtliff ME, Hassett DJ, Parsek MR, Jeffers AK. 2005. The
591 exopolysaccharide alginate protects *Pseudomonas aeruginosa* biofilm bacteria from
592 IFN-gamma-mediated macrophage killing. J Immunol 175:7512-7518.
593 12. Waine DJ, Honeybourne D, Smith EG, Whitehouse JL, Dowson CG. 2008.
594 Association between hypermutator phenotype, clinical variables, mucoid phenotype,
595 and antimicrobial resistance in *Pseudomonas aeruginosa*. J Clin Microbiol 46:3491-
596 3493.
597 13. Cystic fibrosis patient registry annual report 2014. Available from:
598 https://www.cff.org/2014-Annual-Data-Report.pdf.
599 14. Worlitzsch D, Tarran R, Ulrich M, Schwab U, Cekici A, Meyer KC, Birrer P, Bellon G,
600 Berger J, Weiss T, Botzenhart K, Yankaskas JR, Randell S, Boucher RC, Doring G.
601 2002. Effects of reduced mucus oxygen concentration in airway *Pseudomonas*
602 infections of cystic fibrosis patients. J Clin Invest 109:317-325.
603 15. Kirchner S, Fothergill JL, Wright EA, James CE, Mowat E, Winstanley C. 2012. Use
604 of artificial sputum medium to test antibiotic efficacy against *Pseudomonas*
605 *aeruginosa* in conditions more relevant to the cystic fibrosis lung. J Vis Exp
606 doi:10.3791/3857.
607 16. Fung C, Naughton S, Turnbull L, Tingpej P, Rose B, Arthur J, Hu H, Harmer C,
608 Harbour C, Hassett DJ, Whitchurch CB, Manos J. 2010. Gene expression of
609 *Pseudomonas aeruginosa* in a mucin-containing synthetic growth medium mimicking
610 cystic fibrosis lung sputum. J Med Microbiol 59:1089-1100.
611 17. Quinn RA, Whiteson K, Lim Y-W, Salamon P, Bailey B, Mienardi S, Sanchez SE,
612 Blake D, Conrad D, Rohwer F. 2015. A Winogradsky-based culture system shows an
613 association between microbial fermentation and cystic fibrosis exacerbation. ISME J
614 9:1024-1038.
615 18. McCarthy RR, Mooij MJ, Reen FJ, Lesouhaitier O, O'Gara F. 2014. A new regulator
616 of pathogenicity (bvlR) is required for full virulence and tight microcolony formation in
617 *Pseudomonas aeruginosa*. Microbiol 160:1488-1500.

618 19. Windmueller N, Witten A, Block D, Bunk B, Sproeer C, Kahl BC, Mellmann A. 2015.
619 Transcriptional adaptations during long-term persistence of *Staphylococcus aureus* in
620 the airways of a cystic fibrosis patient. International J Med Microbiol 305:38-46.
621 20. Nafee N, Husari A, Maurer CK, Lu C, de Rossi C, Steinbach A, Hartmann RW, Lehr
622 C-M, Schneider M. 2014. Antibiotic-free nanotherapeutics: Ultra-small, mucus-
623 penetrating solid lipid nanoparticles enhance the pulmonary delivery and anti-
624 virulence efficacy of novel quorum sensing inhibitors. J Control Release 192:131-
625 140.
626 21. Yang Y, Tsifansky MD, Wu CJ, Yang HI, Schmidt G, Yeo Y. 2010. Inhalable antibiotic
627 delivery using a dry powder co-delivering recombinant deoxyribonuclease and
628 ciprofloxacin for treatment of cystic fibrosis. Pharm Res 27:151-160.
629 22. Nguyen D, Joshi-Datar A, Lepine F, Bauerle E, Olakanmi O, Beer K, McKay G,
630 Siehnel R, Schafhauser J, Wang Y, Britigan BE, Singh PK. 2011. Active starvation
631 responses mediate antibiotic tolerance in biofilms and nutrient-limited bacteria.
632 Science 334:982-986.
633 23. Filkins LM, O'Toole GA. 2015. Cystic fibrosis lung infections: polymicrobial, complex,
634 and hard to treat. Plos Path 11, doi:10.1371/journal.ppat.1005258.
635 24. Barry PJ, Jones AM. 2015. New and emerging treatments for cystic fibrosis. Drugs
636 75:1165-1175.
637 25. Li J, Nation RL, Turnidge JD, Milne RW, Coulthard K, Rayner CR, Paterson DL.
638 2006. Colistin: the re-emerging antibiotic for multidrug-resistant Gram-negative
639 bacterial infections. Lancet Infect Dis 6:589-601.
640 26. Azzopardi EA, Ferguson EL, Thomas DW. 2013. The enhanced permeability
641 retention effect: a new paradigm for drug targeting in infection. J Antimicrob
642 Chemother 68:257-274.
643 27. Li J, Nation RL, Milne RW, Turnidge JD, Coulthard K. 2005. Evaluation of colistin as
644 an agent against multi-resistant in Gram-negative bacteria. Int J Antimicrob Agents
645 25:11-25.

646 28. Barriere SL. 2015. Clinical, economic and societal impact of antibiotic resistance.
647 Expert Opin Pharmacother 16:151-153.
648 29. Khan S, Tondervik A, Sletta H, Klinkenberg G, Emanuel C, Onsøyen E, Myrvold R,
649 Howe RA, Walsh TR, Hill KE, Thomas DW. 2012. Overcoming drug resistance with
650 alginate oligosaccharides able to potentiate the action of selected antibiotics.
651 Antimicrob Agents Chemother 56:5134-5141.
652 30. Powell LC, Pritchard MF, Emanuel C, Onsøyen E, Rye PD, Wright CJ, Hill KE,
653 Thomas DW. 2014. A nanoscale characterization of the interaction of a novel
654 alginate oligomer with the cell surface and motility of *Pseudomonas aeruginosa*. Am.
655 J Respir Cell Mol Biol 50:483-492.
656 31. Pritchard MF, Powell LC, Menzies GE, Lewis PD, Hawkins K, Wright C, Doull I,
657 Walsh TR, Onsøyen E, Dessen A, Myrvold R, Rye PD, Myrset AH, Stevens HNE,
658 Hodges LA, MacGregor G, Neilly JB, Hill KE, Thomas DW. 2016. A new class of safe
659 oligosaccharide polymer therapy to modify the mucus barrier of chronic respiratory
660 disease. Mol Pharma 13:863-872.
661 32. Hengzhuang W, Song Z, Ciofu O, Onsøyen E, Rye PD, Høiby N. 2016. OligoG CF-
662 5/20 Disruption of Mucoid *Pseudomonas aeruginosa* Biofilm in a Murine Lung
663 Infection Model. Antimicrob Agents Chemother 60:2620-2626.
664 33. Heydorn A, Nielsen AT, Hentzer M, Sternberg C, Givskov M, Ersboll BK, Molin S.
665 2000. Quantification of biofilm structures by the novel computer program COMSTAT.
666 Microbiol 146:2395-2407.
667 34. Morris ER, Rees DA, Sanderson GR, Thom D. 1975. Conformation and circular
668 dichroism of uronic acid residues in glycosides and polysaccharides. J Chem Soc
669 Perk. 2:1418-1425.
670 35. Ciofu O, Tolker-Nielsen T, Jensen PO, Wang H, Høiby N. 2015. Antimicrobial
671 resistance, respiratory tract infections and role of biofilms in lung infections in cystic
672 fibrosis patients. Adv Drug Deliv Rev 85:7-23.

673 36. Sherrard LJ, Tunney MM, Elborn JS. 2014. Antimicrobial resistance in the respiratory
674 microbiota of people with cystic fibrosis. Lancet 384:703-713.
675 37. Ceri H, Olson ME, Stremick C, Read RR, Morck D, Buret A. 1999. The Calgary
676 Biofilm Device: New technology for rapid determination of antibiotic susceptibilities of
677 bacterial biofilms. J Clin Microbiol 37:1771-1776.
678 38. Liu Y-Y, Wang Y, Walsh TR, Yi L-X, Zhang R, Spencer J, Doi Y, Tian G, Dong B,
679 Huang X, Yu L-F, Gu D, Ren H, Chen X, Lv L, He D, Zhou H, Liang Z, Liu J-H, Shen
680 J. 2016. Emergence of plasmid-mediated colistin resistance mechanism MCR-1 in
681 animals and human beings in China: a microbiological and molecular biological
682 study. Lancet Infect Dis 16:161-168.
683 39. Breidenstein EBM, de la Fuente-Nunez C, Hancock REW. 2011. *Pseudomonas*
684 *aeruginosa*: all roads lead to resistance. Trends in Microbiol 19:419-426.
685 40. Nation RL, Li J, Cars O, Couet W, Dudley MN, Kaye KS, Mouton JW, Paterson DL,
686 Tam VH, Theuretzbacher U, Tsuji BT, Turnidge JD. 2015. Framework for
687 optimisation of the clinical use of colistin and polymyxin B: the Prato polymyxin
688 consensus. Lancet Infect Dis 15:225-234.
689 41. Huang JX, Blaskovich MAT, Pelingon R, Ramu S, Kavanagh A, Elliott AG, Butler MS,
690 Montgomery AB, Cooper MA. 2015. Mucin binding reduces colistin antimicrobial
691 activity. Antimicrob Agents Chemother 59:5925-5931.
692 42. Hengzhuang W, Song Z, Ciofu O, Onsøyen E, Rye P, Høiby N. 2013. Biofilm
693 disruption and synergistic antimicrobial effects of a novel alginate oligomer on
694 *Pseudomonas aeruginosa in vivo*. Pediatr Pulmonol 48:294-294.
695 43. Sriramulu DD, Lunsdorf H, Lam JS, Romling U. 2005. Microcolony formation: a novel
696 biofilm model of Pseudomonas aeruginosa for the cystic fibrosis lung. J Med
697 Microbiol 54:667-676.
698 44. Nivens DE, Ohman DE, Williams J, Franklin MJ. 2001. Role of alginate and its O
699 acetylation in formation of *Pseudomonas aeruginosa* microcolonies and biofilms. J
700 Bacteriol 183:1047-1057.

701 45. Garnett JA, Matthews S. 2012. Interactions in bacterial biofilm development: A
702 structural perspective. Curr Protein Pept Sci 13:739-755.
703 46. Billings N, Millan MR, Caldara M, Rusconi R, Tarasova Y, Stocker R, Ribbeck K.
704 2013. The extracellular matrix component Psl provides fast-acting antibiotic defense
705 in *Pseudomonas aeruginosa* biofilms. Plos Path 9, doi:10.1371/journal.ppat.1003526.
706 47. Caballero JD, Clark ST, Coburn B, Zhang Y, Wang PW, Donaldson SL, Tullis DE,
707 Yau YCW, Waters VJ, Hwang DM, Guttman DS. 2015. Selective sweeps and parallel
708 pathoadaptation drive *Pseudomonas aeruginosa* evolution in the cystic fibrosis lung.
709 mBio 6, doi:10.1128/mBio.00981-15
710 48. Carroll SM, Lee M-C, Marx CJ. 2014. Sign epistasis limits evolutionary trade-offs at
711 the confluence of single- and multi-carbon metabolism in *Methylobacterium*
712 *Extorquens* AM1. Evolution 68:760-771.
713 49. Jiang P, Li J, Han F, Duan G, Lu X, Gu Y, Yu W. 2011. Antibiofilm Antibiofilm activity
714 of an exopolysaccharide from marine bacterium *Vibrio* sp QY101. Plos One 6:1-11.
715 50. Alipour M, Suntres ZE, Omri A. 2009. Importance of DNase and alginate lyase for
716 enhancing free and liposome encapsulated aminoglycoside activity against
717 *Pseudomonas aeruginosa*. J Antimicrob Chemother 64:317-325.
718 51. Alkawash MA, Soothill JS, Schiller NL. 2006. Alginate lyase enhances antibiotic
719 killing of mucoid *Pseudomonas aeruginosa* in biofilms. APMIS 114:131-138.
720 52. Lembre P, Lorentz Cc, Di Martino P. 2012. Exopolysaccharides of the biofilm matrix:
721 A complex biophysical world. INTECH Open Access Publisher, doi: 10.5772/51213.
722 Available from: http://www.intechopen.com/books/the-complex-world-of-
723 polysaccharides/exopolysaccharides-of-the-biofilm-matrix-a-complex-biophysical-
724 world
725 53. Flemming H.C, Wingender J. 2010. The biofilm matrix. Nat Rev Microbiol 8:623-633.
726 54. Aslam SN, Newman MA, Erbs G, Morrissey KL, Chinchilla D, Boller T, Jensen TT,
727 De Castro C, Ierano T, Molinaro A, Jackson RW, Knight MR, Cooper RM. 2008.

728 Bacterial polysaccharides suppress induced innate immunity by calcium chelation.
729 Curr Biol 18:1078-1083.
730 55. Martinez-Gomez F, Mansilla A, Matsuhiro B, Matulewicz MC, Troncoso-Valenzuela
731 MA. 2016. Chiroptical characterization of homopolymeric block fractions in alginates.
732 Carbohydr Polym 146:90-101.
733 56. Grant GT, Morris ER, Rees DA, Smith PJC, Thom D. 1973. Biological interactions
734 between polysaccharides and divalent cations: The egg-box model. FEBS Lett.
735 32:195-198.
736 57. De Soyza A, Hall AJ, Mahenthiralingam E, Drevinek P, Kaca W, Drulis-Kawa Z,
737 Stoitsova SR, Toth V, Coenye T, Zlosnik JEA, Burns JL, Sa-Correia I, De Vos D,
738 Pirnay J-P, Kidd TJ, Reid D, Manos J, Klockgether J, Wiehlmann L, Tuemmler B,
739 McClean S, Winstanley C, BM EFFCA. 2013. Developing an international
740 *Pseudomonas aeruginosa* reference panel. MicrobiologyOpen 2:1010-1023.
741 58. Ravn L, Christensen AB, Molin S, Givskov M, Gram L. 2001. Methods for detecting
742 acylated homoserine lactones produced by Gram-negative bacteria and their
743 application in studies of AHL-production kinetics. J Microbiol Methods 44:239-251.

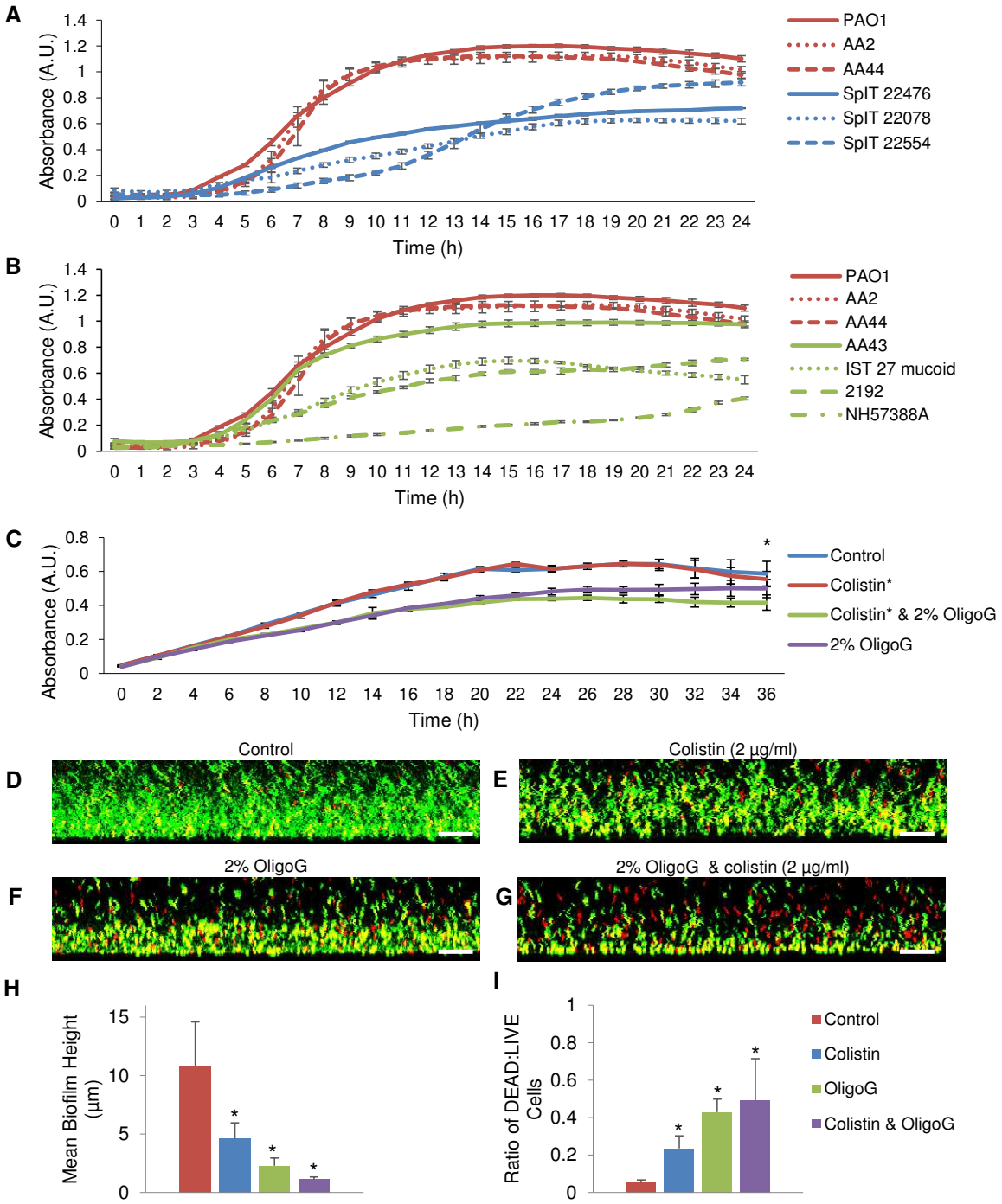

FIG 1 Comparison of planktonic growth in MH medium of characterized and new cystic fibrosis *P. aeruginosa* isolates and biofilm growth following antimicrobial treatment. Growth curves (24 h) of (A) Non-mucoid IPARP isolates (red) versus fresh clinical SpIT isolates (blue) and (B) non-mucoid IPARP isolates (red) versus mucoid (green). (C) Growth curves of NH57388A (36 h) ± 2% and OligoG CF-5/20 with/without colistin (0.05 µg/ml). Biofilm disruption assay showing LIVE/DEAD® CLSM [scale bar 20 µm] of 24 h established NH57388A biofilms, (D) untreated control, (E) 1 h colistin treatment, (F) 2% OligoG CF-5/20, (G) combined treatment. COMSTAT analysis showing (H) mean height of biofilm and (I) ratio of DEAD: LIVE cells. (*p<0.05)

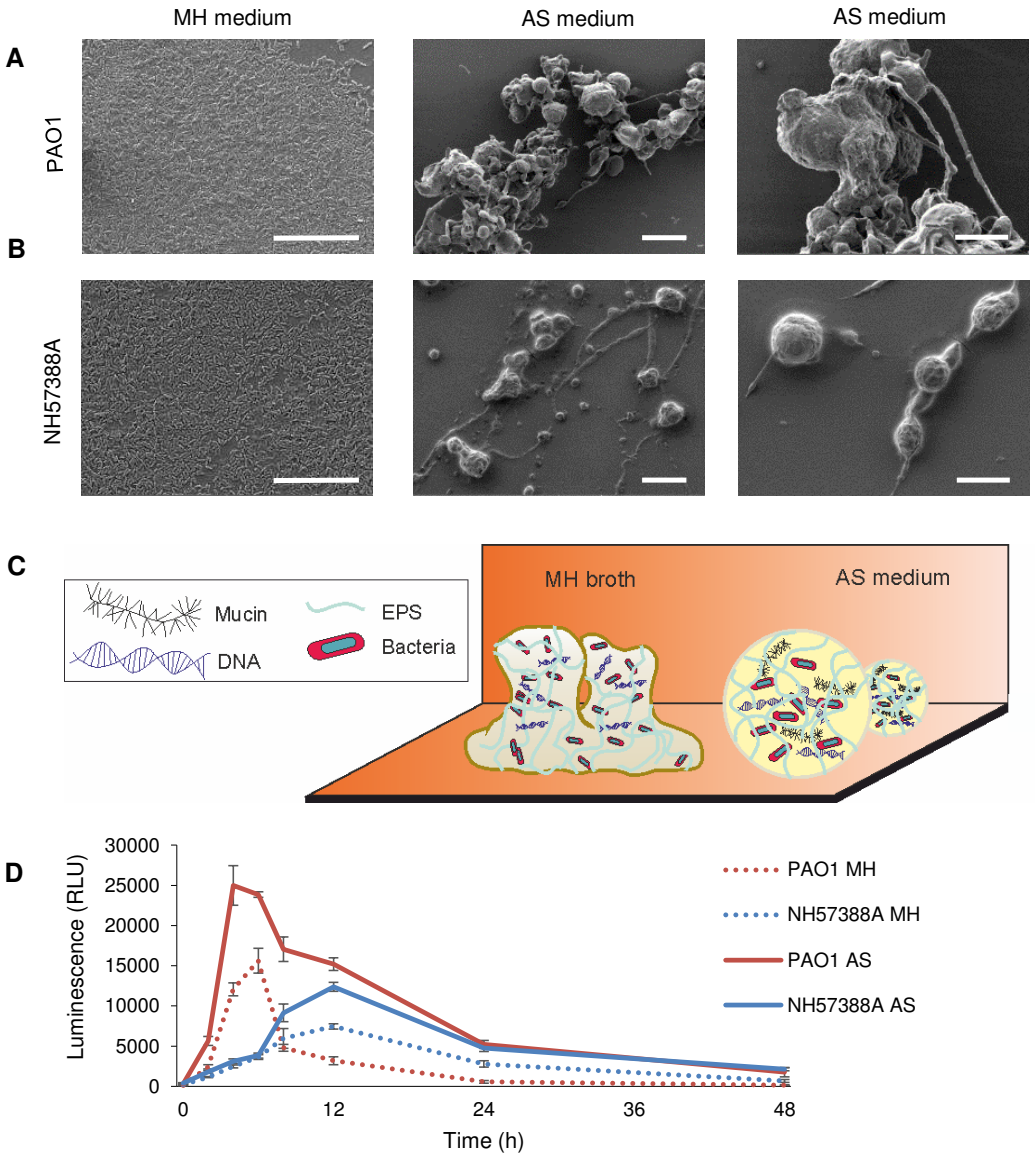

FIG 2 Comparison of growth of non-mucoid PAO1 and mucoid NH57388A *P. aeruginosa* in Mueller-Hinton (MH) and artificial sputum (AS) medium. Scanning electron microscopy of bacterial growth in MH (24 h) and AS medium (48 h; scale bar 20 µm), with corresponding 'zoomed-in' images in AS medium [scale bar 10 µm] (A) PAO1 and (B) NH57388A. (C) Diagrammatic representation of biofilm structure in both media. (D) Cell viability (ATP production) of *P. aeruginosa* NH57388A and PAO1 (10^8 cfu/ml) grown in MH and AS medium.

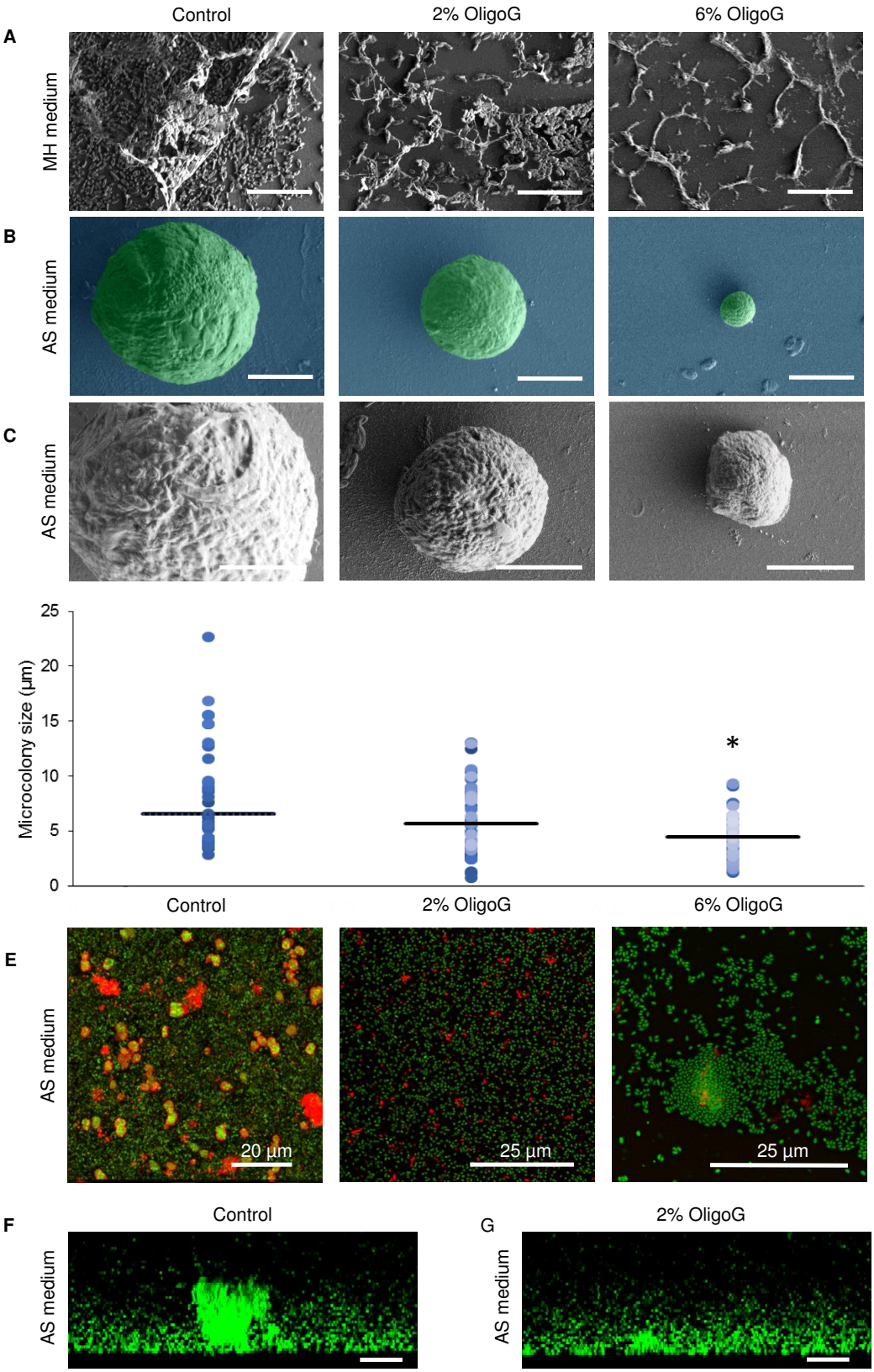

FIG 3 Biofilm formation assays showing mucoid NH57388A *P. aeruginosa* biofilms grown in Mueller-Hinton (MH) and artificial sputum (AS) medium. SEM images of *P. aeruginosa* (NH57388A) biofilms grown ±OligoG CF-5/20 for (A) 24 h in Mueller Hinton (MH) medium; 10 µm; (B), (C [zoomed in]) 48 h ± OligoG CF-5/20 [scale bar 5 µm] with (D) corresponding scatter graphs showing approx. mean microcolony size. (E) Corresponding CLSM EPS staining of *P. aeruginosa* (NH57388A) 48 h biofilms in artificial sputum (AS) medium using Syto-9 (green) and Concanavalin A 633 (red). (F,G) Biofilm disruption assay using Syto-9 (green) showing cross-sectional views of 48 h established biofilms treated I h with 2% OligoG CF-5/20 [scale bar 10 µm]. (*$p<0.05$).

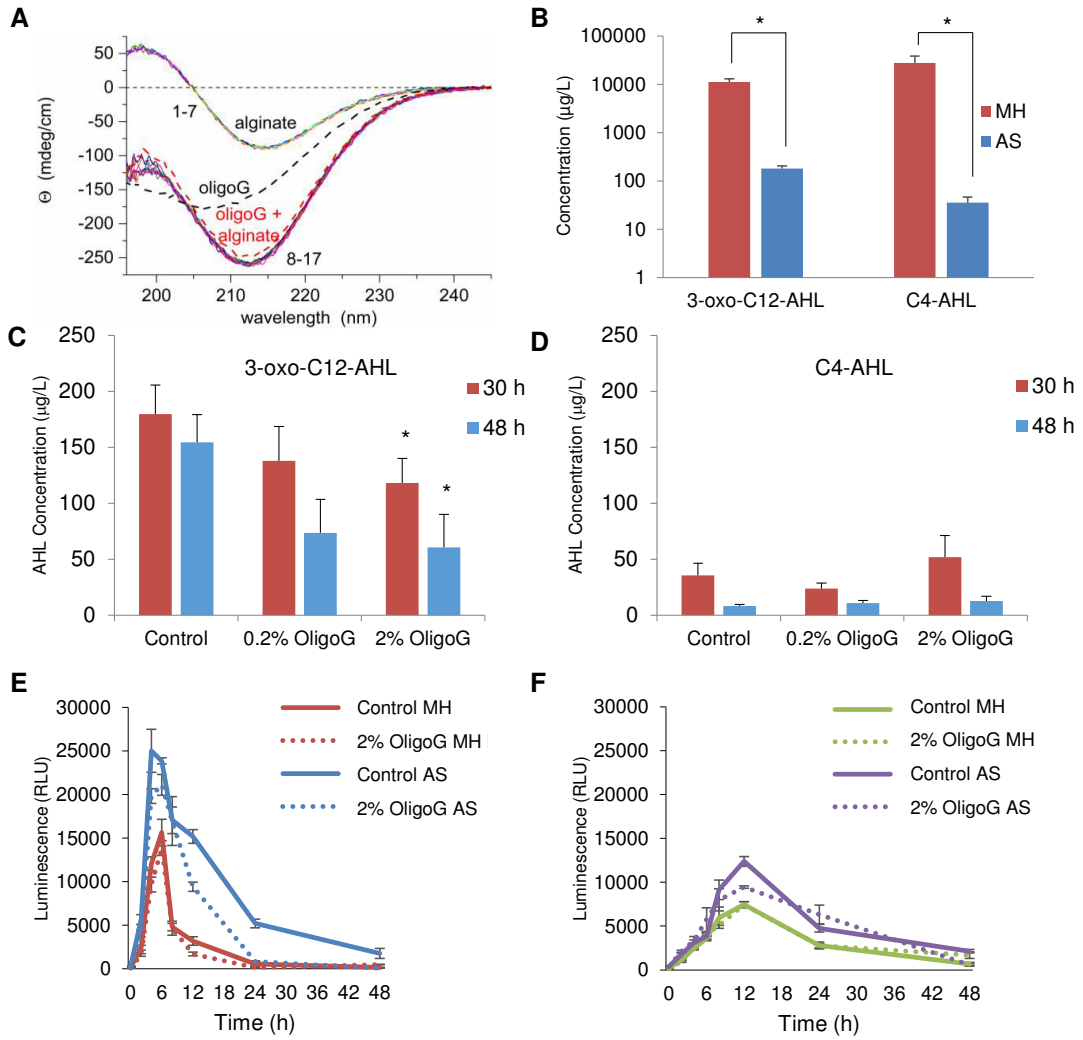

FIG 4 Effect of OligoG CF-5/20 on high Mw alginate and on cell signaling molecules *in vitro*. (A) Circular dichroism (CD) spectra of high Mw pseudomonal alginate mixed with OligoG CF-5/20. Scans 1-7 show spectra of high Mw alginate (~20 µM) followed over ~77 min upon heating from 4 to 37^{0}C; scans 8-11 (~44min) are recorded after addition of OligoG CF-5/20 (850 µM) followed by addition of Ca^{2+} (1mM) (scans 12-17, ~ 66min). Spectra of OligoG CF-5/20 (850 µM) alone and its sum with high Mw alginate (20 µM) are shown as black and red dashed lines, respectively. High performance liquid chromatography (HPLC) mass spectrometry (LC-QQQ-MS) to quantify acyl homoserine lactone (AHL; 3-oxo-C12-AHL and C4-AHL) production of *P. aeruginosa* PAO1 (B) grown in MH and AS medium (30 h), and in a time course assay (30 and 48 h) showing the effect of OligoG CF-5/20 on (C) 3-oxo C12-AHL and (D) C4-AHL (*$p<0.05$; n=3). Cell viability (ATP production) over 48 h of (E) PAO1 and (F) NH57388A grown in MH and AS medium ± 2% OligoG CF-5/20 (2%G).

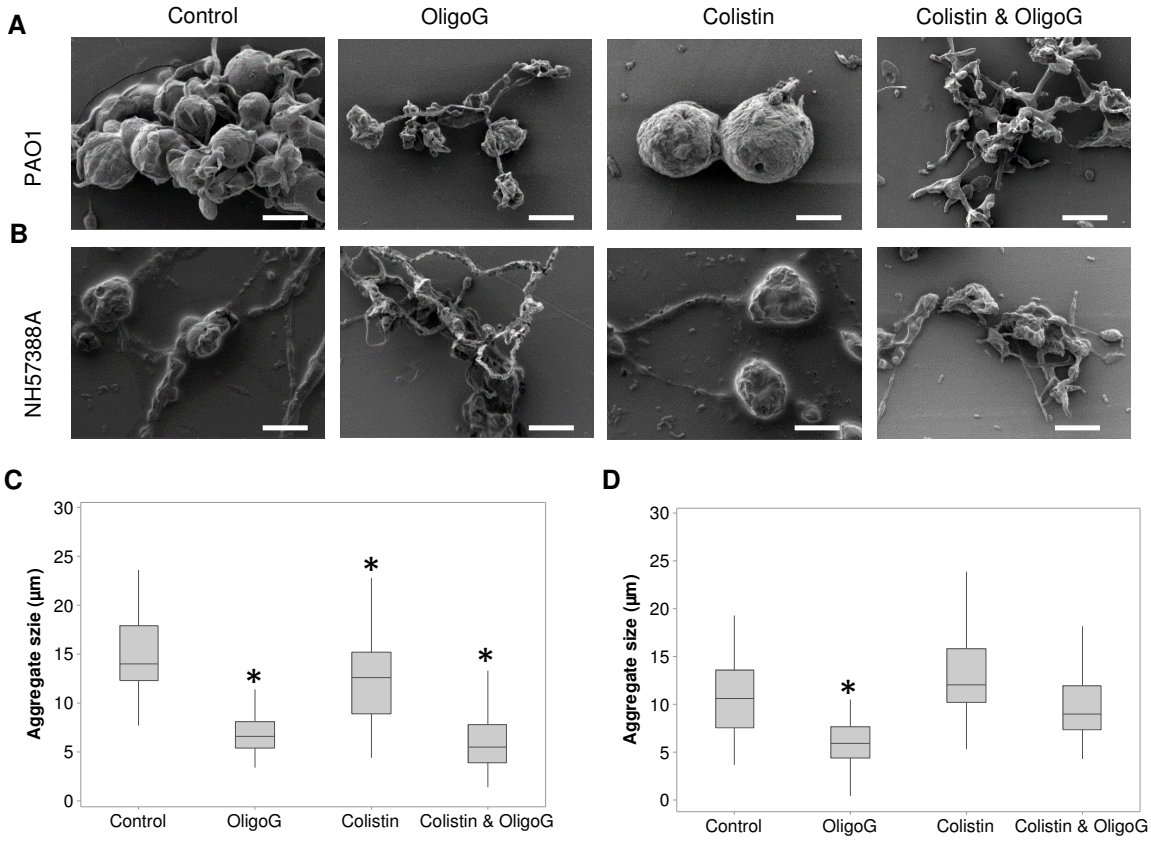

FIG 5 Biofilm disruption assays showing scanning electron microscopy (SEM) of antimicrobial (OligoG CF 5/20 and colistin) treated biofilms grown in ASM [Scale bar 10 µm]. SEM images of established (24 h) *P. aeruginosa* (A) PAO1 and (B) NH57388A biofilms treated for 24 h with 2% OligoG CF-5/20 ± colistin (16 µg/ml) with corresponding median microcolony diameter measurements for (C) PAO1 and (D) NH57388A (*$p<0.05$).